Molecular Cloning and Characterization of the von Hippel-Lindau-Like Protein

Heng Qi,[1] Michelle L. Gervais,[1] Wei Li,[2] James A. DeCaprio,[3] John R.G. Challis,[2] and Michael Ohh[1]

[1]Department of Laboratory Medicine and Pathobiology and [2]Department of Obstetrics and Gynecology, University of Toronto, Toronto, Ontario, Canada; and [3]Department of Molecular Oncology, Dana-Farber Cancer Institute, Harvard Medical School, Boston, MA

Abstract

von Hippel-Lindau (VHL) tumor suppressor protein—inactivated in VHL disease and sporadic kidney cancer—is a component of an E3 ubiquitin ligase complex that selectively ubiquitinates the α subunit of the hypoxia-inducible factor (HIF) transcription factor for subsequent destruction by the 26S proteasome. Here, we report the identification and characterization of the first *VHL* homologue, *VHL-like protein* (*VLP*), located on chromosome 1q21.2. A 676-bp partial cDNA encoding a 139-amino acid protein that is 78% similar to VHL was isolated by reverse transcription-PCR from human brain cerebellum and several cancer cell lines. The expression of *VLP* transcript is most abundant in the placenta. Like VHL, VLP contains a β domain capable of binding HIFα. However, unlike VHL, it does not contain a recognizable α domain, which is required for nucleating the multiprotein E3 ubiquitin ligase complex. The increased expression of VLP in the presence of VHL attenuated the ubiquitination of HIFα and led to the accumulation of downstream HIF target genes. These results taken together indicate that VLP functions as a dominant-negative VHL to serve as a protector of HIFα.

Introduction

Functional inactivation of von Hippel-Lindau (VHL) is the cause of VHL disease and the majority of sporadic renal clear cell carcinoma, the most common form of kidney cancer (1, 2). Individuals with the VHL disease develop hypervascular tumors in multiple organs including the central nervous system (brain and spine), retina, pancreas, adrenal gland, endolymphatic sac of the inner ear, and kidney (1, 2). Certain mutations in VHL also cause congenital polycythemia (3, 4). These VHL disease-associated phenotypes have been attributed to the inability to down-regulate hypoxia-inducible factor α (HIFα) during normoxia, and the consequential inappropriate up-regulation of hypoxia-inducible genes such as vascular endothelial growth factor (*VEGF*), glucose transporter 1 (*GLUT1*), transferrin (*TF*), transferrin receptor (*TFRC*), and erythropoietin (*EPO*; 1).

It is now evident that VHL is a vital component of a multiprotein E3 ubiquitin ligase complex that consists of elongin B, elongin C, Rbx1, and Cul2 (1, 5, 6). VHL contains an α domain and a β domain (7). The former is required for binding elongin C, thereby bridging VHL to the rest of the E3 complex (7, 8). The latter functions as a putative substrate-docking site that directly binds HIFα (7, 9). However, oxygen-dependent hydroxylation of conserved proline residues within the oxygen-dependent degradation (ODD) domain of HIFα by a class of prolyl hydroxylases (PHD) is a requisite step in this recognition by VHL (10–15). Thus, under normal oxygen tension, VHL ubiquitin ligase complex selectively ubiquitinates the prolyl-hydroxylated form of HIFα. Importantly, the disease-associated VHL mutants are unable to target the prolyl-hydroxylated HIFα for ubiquitin-mediated proteolysis due to their failure to form an active E3 complex (*i.e.*, α domain mutation) or to their inability to recognize prolyl-hydroxylated HIFα (*i.e.*, β domain mutation; 9, 16, 17). Consequently, cells lacking a wild-type VHL show stable HIFα subunits, which binds to the constitutively non-labile HIFβ [also known as ARNT (aryl-hydrocarbon receptor nuclear translocator)] subunit. This active heterodimeric transcription factor induces the transcription of numerous hypoxia-inducible genes, such as the aforementioned *VEGF*, *EPO*, *TF*, *TFRC*, and *GLUT1*, and initiates an inappropriate physiological response to hypoxia (1).

Oxygen homeostasis is paramount for the normal functioning of a cell. It follows then that the mechanisms governing oxygen homeostasis is not only precise, but also complex, occurring at multiple levels. First, there are multiple α subunits of HIF: HIF-1α, HIF-2α, and HIF-3α, all capable of transactivating promoters/enhancers containing hypoxia-responsive elements (HRE; 18–24). Second, under normal oxygen tension, prolyl hydroxylation on HIFα promotes the binding of VHL E3 ubiquitin complex (12, 14, 15), while asparaginyl hydroxylation on HIFα prevents the binding of transcriptional coactivators CBP/p300 (25). This dual posttranslational regulation safeguards against inappropriate activation of hypoxia-inducible genes under normal oxygen tension. Recently, a dominant-negative regulator of murine HIF-1 called mIPAS (murine inhibitor of PAS containing proteins), which lacks transactivation and ODD domains, was identified as an alternatively spliced variant of mHIF-3α (20, 21). mIPAS dimerizes with mHIF-1α subunit and consequently prevents the interaction of

Received 5/15/03; revised 12/4/03; accepted 12/8/03.
The costs of publication of this article were defrayed in part by the payment of page charges. This article must therefore be hereby marked advertisement in accordance with 18 U.S.C. Section 1734 solely to indicate this fact.
Grant support: National Cancer Institute of Canada with funds from the Terry Fox Foundation (Grant no. 13030). H.Q. is a recipient of the Canadian Institutes of Health Research (CIHR) fellowship.
Note: M.O. is a Canada Research Chair in Molecular Oncology.
Requests for reprints: Michael Ohh, Department of Laboratory Medicine and Pathobiology, University of Toronto, 1 King's College Circle, Toronto, Ontario, M5S 1A8 Canada. Phone: (416) 946-7922; Fax: (416) 978-5959.
E-mail: michael.ohh@utoronto.ca

mHIF-1α to mHIF-β subunits (20, 21). Furthermore, mIPAS/mHIF-1α complex does not bind to the HRE of target genes (20, 21). Thus, mIPAS inhibits hypoxia-mediated transcriptional activation. Adding to the complexity of mechanisms governing oxygen homeostasis, we report here the identification and functional characterization of the first *VHL* homologue, *VHL-like protein* (*VLP*).

Results and Discussion

Molecular Cloning of VLP

A recent GenBank cDNA entry (Accession No.: XM_089387) encoded a protein similar to VHL. This cDNA sequence mapped to a human genomic DNA sequence from clone RP11-443G18 (Accession No.: AL589685) on chromosome 1q21.2 between markers D1S2721 and D1S2635. On the basis of the cDNA and genomic DNA sequences, we performed reverse transcription (RT)-PCR on total RNA isolated from cells derived from various tissue types, such as 786-O (kidney), SAOS-2 (bone), HepG2 (liver), and MCF7 (breast). Sequencing of the PCR products generated from these cells confirmed an identical cDNA of 676 bp (Fig. 1A). This cDNA contained an additional 110 bp extending upstream of the 5′ end of XM_089387, as well as an additional 104 bp (corresponding to nucleotides 448–551) that is absent in XM_089387 (Fig. 1B). The predicted open reading frame (ORF) of our 676-bp cDNA encodes a putative 139-amino acid protein that is 67.6% identical and 78% similar to the amino acids 1–157 of VHL protein (Fig. 1C). We have, therefore, designated this gene as *VLP* (Accession No.: AY494836). VLP contains a highly conserved putative substrate-docking β domain (represented by a *solid line* in Fig. 1C) but does not contain an α domain required for nucleating an E3 ligase complex (represented by a *dashed line* in Fig. 1C).

It should be noted that the absence of an α domain in VLP is caused by a frameshift due to one base insertion and one base deletion in the *VLP* gene and not due to the lack of nucleotides corresponding to the exon 3 of *VHL*. This raises the possibility that a frameshift mutation is observed in certain cancer cell lines, but may not be present in normal cells. A blast search of the GenBank revealed a 5′ EST isolated from human brain cerebellum (Accession No.: AA324790) located upstream of the presented *VLP* cDNA. This EST sequence overlapped with *VLP* cDNA by 24 bp and contained an in-frame stop codon (−69 to −67) upstream of the first methionine codon (Fig. 1B), suggesting the expression of VLP in human brain cerebellum. We performed RT-PCR using RNA extracted from the human brain cerebellum and amplified an identical 676-bp cDNA. A negative control without reverse transcriptase did not generate the 676-bp fragment, suggesting that the RT-PCR amplicons were not generated from a contaminating genomic DNA. This result supports the notion that VLP is naturally missing an α domain.

Bradley and Rothberg (26) previously reported a partial 218-bp DNA fragment, which is possibly a *VHL*-processed pseudogene. This DNA fragment is identical to the nucleotides 186–403 of presented *VLP* cDNA. Northern analysis was performed on several human tissue types and they found that the probe of this *VHL*-processed pseudogene cross-hybridized with *VHL* mRNA transcripts and showed no unique transcript. We have performed similar Northern analysis on multiple human tissue blot using the *VLP* coding sequence (from 111 to 530) and *VHL* coding region as probes. Although both probes showed common transcripts at 4.5 kb (Fig. 2A), the 3- and 1-kb transcripts in the placenta were detected only by the *VLP* probe (Fig. 2A). This strongly suggests the existence of *VLP* mRNA in the placenta. It is likely that the 218-bp probe used by Bradley and Rothberg, which contained just 48 mismatches (while our probe contained 145 mismatches) against the VHL cDNA, was insufficient to provide the unique Northern signature of VLP.

We have also identified in the database a putative murine *VLP* homologue, *mVLP* (XM_139939; Fig. 1C). This sequence was derived by automated computational analysis using the GNOMON gene prediction method. The predicted ORF encodes a 131-amino acid protein. At the predicted protein level, mVLP is 56% identical to the human VLP. mVLP contains a fairly well-conserved β domain and a grossly truncated α domain (Fig. 1C).

We next asked whether VLP protein is expressed in the placenta. In the absence of anti-VLP antibody, we tested the existing anti-VHL antibodies to determine whether they cross-react with VLP due to the high degree of similarity between the two proteins (Fig. 2B). ^{35}S-*in vitro* translated hemagglutinin (HA)-VLP was immunoprecipitated with both monoclonal (IG32) and polyclonal (R98) anti-VHL antibody, separated on SDS-PAGE, and visualized by autoradiography. R98 immunoprecipitated HA-VLP, albeit at a lower affinity than the anti-HA antibody, while IG32 failed to immunoprecipitate HA-VLP (Fig. 2B). Next, we prepared whole cell extracts of primary placental tissue, ran on SDS-PAGE along with *in vitro* translated untagged-VLP, and immunoblotted with R98 antibody (Fig. 2C). A band co-migrating with the untagged-VLP was present in the lane loaded with placental extract, strongly suggesting that the *VLP* mRNA detected via Northern analysis translated into VLP protein in the placenta. Furthermore, this protein was clearly not VHL because it did not co-migrate with VHL proteins (full-length VHL30 or internally translated VHL19) that were immunoprecipitated from ACHN cells that express endogenous VHL (see *lanes 3* and *4* in Fig. 2C). Moreover, the protein band representing VLP in the placenta did not hybridize against the IG32 anti-VHL antibody, suggesting that this is not an alternatively spliced or modified VHL (data not shown). It should nevertheless be cautioned that in the absence of VLP-specific antibody, it is formally possible that the protein representing VLP in the placenta is yet another protein that cross-reacts with an anti-VHL polyclonal antibody.

VLP Binds to the α Subunit of HIF, but Fails to Associate With VHL-Associated E3 Ubiquitin Ligase Components

The substrate-docking β domain of VHL binds HIF-1/2/3α via the ODD domain (7, 9, 22). This recognition requires, at a minimum, oxygen-dependent hydroxylation of a conserved proline residue within the ODD (12, 14, 15). To address whether the putative β domain of VLP could likewise bind ODD of HIF-1α, we performed an *in vitro* binding assay between *in vitro* translated ^{35}S-labeled HA-tagged VLP and *in vitro*

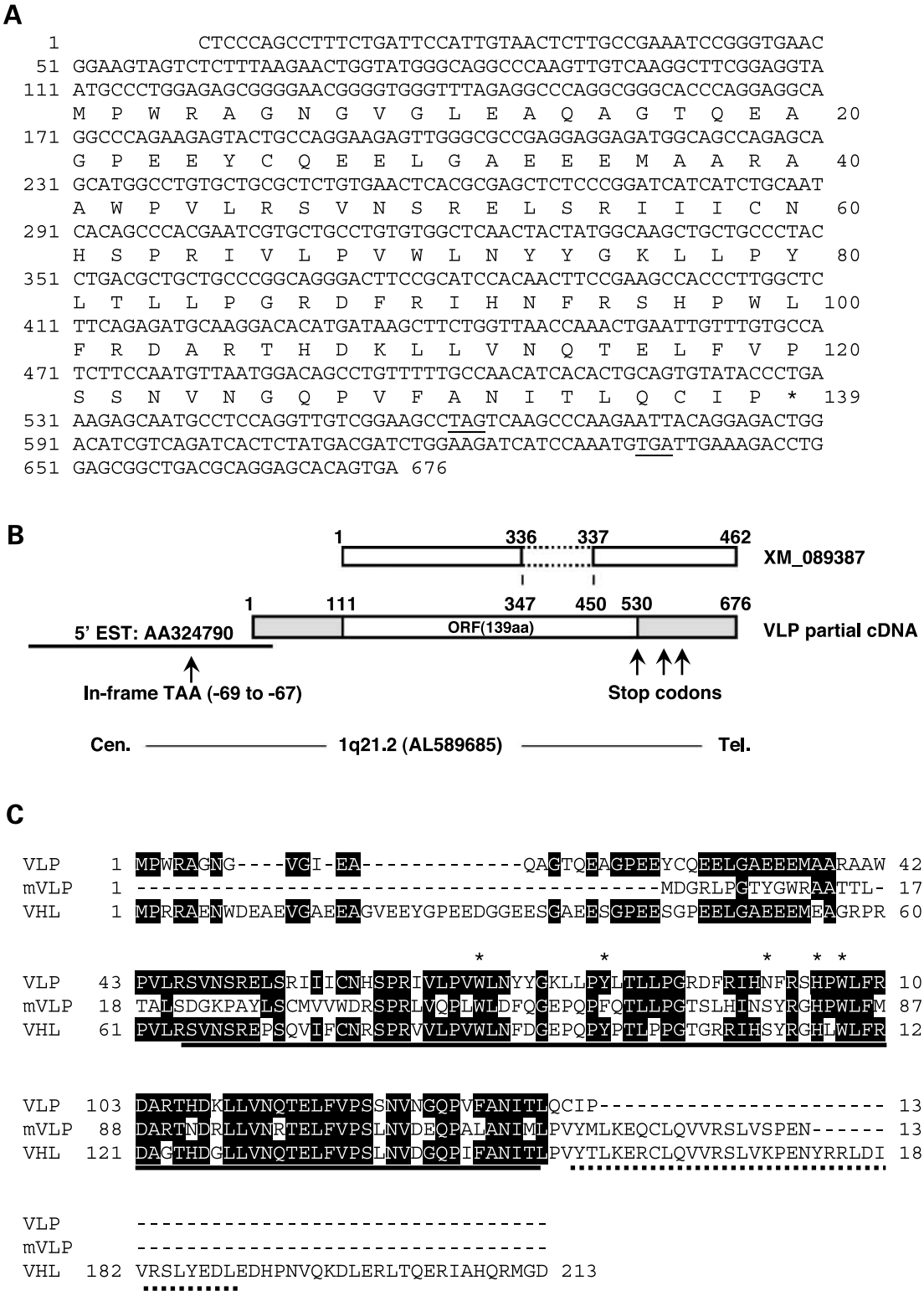

FIGURE 1. Primary sequence and protein alignment of VLP. **A.** Nucleotide and deduced amino acid sequence of VLP. Identical sequence of RT-PCR generated from human brain cerebellum as well as multiple cancer cell lines is 676 bp and contains an ORF of 139 amino acids. The numbers on the *left* indicate the nucleotide number, whereas amino acids are numbered on the *right*. The first methionine is supported by a strong Kozak sequence. *Asterisk* indicates the termination codon. The other two in-frame termination codons in the 3′ untranslated region are *underlined*. **B.** ESTs (Expressed Sequence Tags) matching or overlapping with *VLP*. ORF is shown as *open boxes*; the untranslated region is shown as *gray boxes*. The termination codons are indicated. **C.** Alignment of human VLP, putative murine mVLP, and VHL amino acid sequences. *Shaded boxes* indicate identical residues. *Solid* and *dashed lines* indicate the β and α domains of VHL, respectively. *Asterisks* (above the amino acids) indicate key residues of VHL that make direct contact with HIF-1α(ODD).

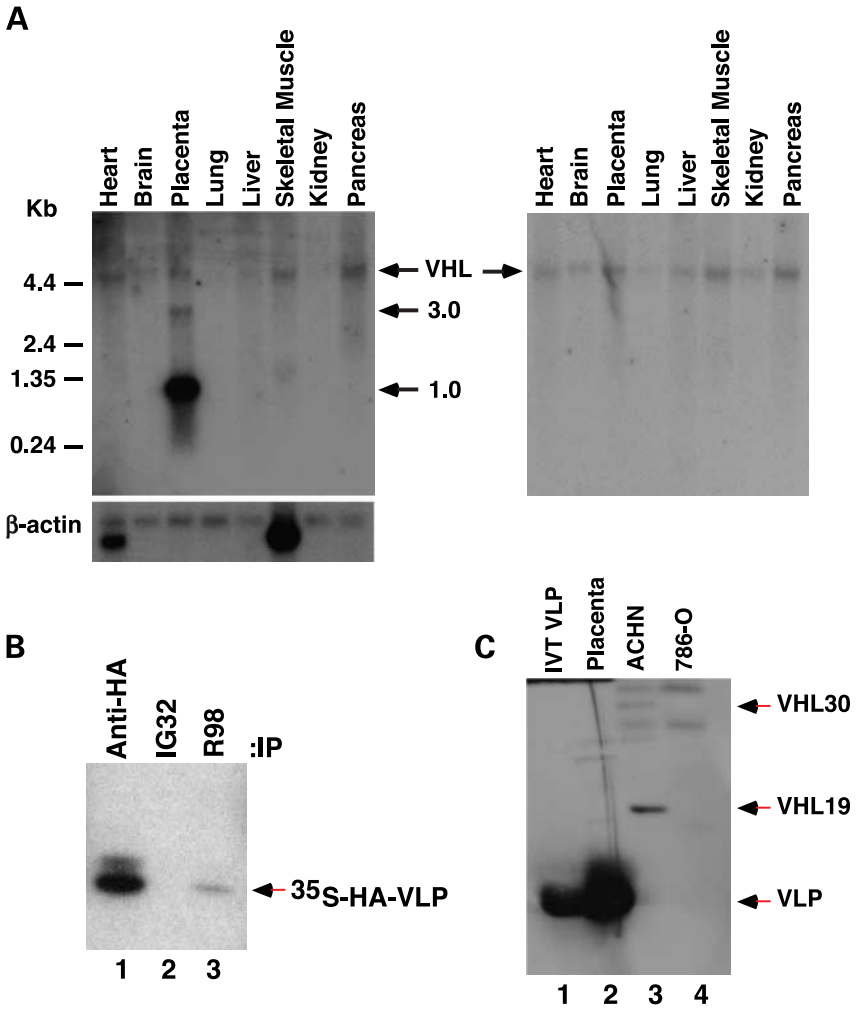

FIGURE 2. Tissue distribution pattern of VLP. **A.** Human tissue Northern blot was developed using ^{32}P-labeled *VLP* cDNA derived from *Bam*HI/*Eco*RI fragment of pcDNA3-HA-VLP (*left panel*) or ^{32}P-labeled *VHL* cDNA derived from *Bam*HI/*Eco*RI fragment of pcDNA3-T7-VHL (*right panel*). Cross-hybridizing *VHL* transcripts are indicated as bands corresponding to the longest transcripts. *Arrows* at 3 and 1 kb are *VLP* mRNA transcripts. *Lower panel* shows the β-actin transcript expression. **B** and **C.** VLP expression in primary placenta. **B.** ^{35}S-*in vitro* translated HA-tagged VLP was immunoprecipitated with anti-HA, anti-VHL monoclonal (*IG32*), or anti-VHL polyclonal (*R98*) antibodies. Bound proteins were separated on SDS-PAGE and visualized by autoradiography. **C.** *In vitro* translated untagged-VLP, whole cell extracts of primary placenta, and anti-VHL immunoprecipitates from ACHN (expresses endogenous VHL: full-length VHL30 and internally translated VHL19), and 786-O (VHL−/−) cells were separated on SDS-PAGE and immunoblotted with anti-VHL polyclonal (R98) antibody.

translated unlabeled ODD(WT) or ODD(P-A) containing P564A substitution, in the presence of PHD-enriched cellular extracts (Fig. 3A). VHL was analyzed in the experiment as an internal control. ODD(WT) clearly bound VLP and, as expected, VHL. However, unlike VHL, VLP bound equally well to ODD(P-A) (Fig. 3A). This suggests that VLP recognizes ODD irrespective of its prolyl hydroxylation status.

We next performed an analogous experiment using a biotin-conjugated ODD-derived synthetic peptide that represents HIF-1α residue 556–575. The ODD peptide-(OH) contains hydroxyproline at position 564, while ODD peptide (P-A) contains a proline to alanine substitution at that position. These biotin-conjugated peptides were mixed with either ^{35}S-labeled VHL or VLP, precipitated with streptavidin-coated beads, and visualized by autoradiography (Fig. 3B). Although VHL bound only to ODD peptide-(OH), VLP bound both ODD peptide-(OH) and ODD peptide (P-A) with relatively equal affinity (Fig. 3B). This was recapitulated in an *in vitro* binding assay using full-length HIF-1α protein (Fig. 3C). The full-length HIF-1α bound VLP, but failed to bind HIF-1α devoid of ODD (Fig. 3C). This suggests that P402, which has also been implicated in regulating the binding to VHL, is not required for binding VLP. However, because HIF-1α devoid of ODD is a gross deletion mutant that might have aberrant conformation, it is still formally possible that P402 plays a minor role in regulating the binding of VLP. Furthermore, as observed with ODD or ODD-derived synthetic peptides, HIF-1α with P564A retained its ability to bind VLP. These results, taken together, strongly suggest that VLP recognizes HIF-1α via ODD independent of its prolyl hydroxylation status. It should, however, be noted that the binding of VLP to HIF-1α(ODD) was noticeably weaker than VHL to HIF-1α(ODD).

HIF-1α(ODD) makes five key contacts on VHL at residues W88, Y98, S111, H115, and W117 (27). S111 and H115 are critical residues of the hydrophobic core within the β domain of VHL that most likely associate with the hydroxyproline of ODD (27). This is thought to be central to the specificity of VHL binding to HIF-1α. Interestingly, 4 out of these 5 residues are conserved on VLP (Fig. 1C). The exception, the residue corresponding to S111 of VHL, is N93 on VLP (Fig. 1C). This and other differences in residues surrounding the key contact sites may be the reason why VLP does not preferentially bind to the prolyl-hydroxylated HIF-1α(ODD). To test this hypothesis, we generated VHL with ^{111}SYRG^{114} to

NFRS substitution and VLP with ^{92}NFRS^{95} to SYRG substitution. These mutants were tested for their ability to bind biotin-conjugated ODD peptide-(OH) and ODD peptide (P-A) (Fig. 3D). VHL (SYRG to NFRS) mutant bound not only ODD peptide-(OH), but also ODD peptide (P-A) (Fig. 3D). Thus, this VHL mutant had a binding profile similar to that of the wild-type VLP. The VLP (^{92}NFRS^{95} to SYRG) mutant, unlike its wild-type counterpart, bound more preferentially to ODD peptide-(OH) (Fig. 3D). Thus, this binding profile was reminiscent of the wild-type VHL requiring the hydroxylation of proline on ODD for recognition. Although the binding affinity was markedly lower than their wild-type counterparts (data not shown), these results demonstrate that subtle amino acid differences surrounding S111 and H115 (position numbers on VHL) are important in determining the specificity of binding to prolyl-hydroxylated HIF-1α(ODD). Interestingly, S111, H115, and the residues in between (*i.e.*, SYRGH) are perfectly conserved on mVLP (see Fig. 1C). Whether mVLP preferentially recognizes prolyl-hydroxylated HIF-1α, like VHL and unlike human VLP, remains to be determined.

The primary sequence indicates that the α domain, which is required for bridging VHL to elongins B/C, Cul2, and Rbx1 (7–9), is absent in VLP (see Fig. 1C). To explore whether VLP is incapable of forming a VHL-like E3 ubiquitin ligase complex, we transiently transfected U2OS cells with mammalian expression plasmid encoding HA-VLP or HA-VHL as a control. The cells were then lysed, immunoprecipitated with an anti-HA antibody, and the bound proteins were separated on SDS-PAGE (Fig. 3E). As expected, VHL co-immunoprecipitated Cul2, a scaffold protein of the VHL E3 complex. However, VLP failed to co-precipitate Cul2 (Fig. 3E). This suggests that VLP without an α domain lacks the ability to bind the components of the VHL E3 ligase complex.

VLP Functions as a Dominant-Negative VHL

Although VLP did not associate with VHL-associated proteins, it was formally possible that VLP could interact with other proteins to act as an E3 ubiquitin ligase to target HIF-1α for ubiquitination. To verify this possibility, we performed an *in vitro* HIF-1α(ODD) ubiquitination assay (Fig. 4A). ^{35}S-labeled HIF-1α(ODD) was ubiquitinated robustly in the presence of VHL (Fig. 4A, *lane 3*). However, the addition of VLP in S100 extracts devoid of VHL had very minimal or undetectable E3 ligase activity (Fig. 4A, *lane 2*). The addition of *in vitro* translated VLP to S100 extracts containing wild-type VHL attenuated the ability of VHL to ubiquitinate HIF-1α(ODD) in a dosage-dependent manner (Fig. 4A, *lanes 4–6*). These results indicate that VLP functions as a dominant-negative VHL and protects HIF-1α from ubiquitin-mediated proteolysis.

We next asked whether VLP can bind endogenous HIF-1α and whether the increased expression of VLP *in vivo* could block VHL-dependent ubiqutin-mediated destruction of HIF-1α and thereby promote the accumulation of hypoxia-inducible products, such as GLUT1. Multiple stable subclones of U2OS cells *(VHL+/+)* expressing either empty plasmid or plasmid-expressing HA-VLP were generated. First, the endogenous HIF-1α co-precipitated with HA-VLP during an anti-HA immunoprecipitation (Fig. 4B). Second, as predicted from our *in vitro* study, mock-transfected cells that express wild-type VHL showed low HIF-1α and GLUT1 levels, while increased expression of VLP resulted in the accumulation of HIF-1α, and consequently overexpressed GLUT1 (Fig. 4, C and D). These results strongly suggest that VLP acts to protect HIF-1α by competing against the destructive targeting initiated by VHL *in vivo*.

VHL is a vital component of an E3 ubiquitin ligase complex. Within this multiprotein enzyme, VHL functions as an F-box protein to specifically recognize and bind its substrate, prolyl-hydroxylated HIF-1, 2, and various splice variants of 3α subunits (12, 14, 15, 22). This posttranslational modification of HIFα only occurs in the presence of oxygen and requires the activity of HIF-specific PHD (10, 11, 13, 22). Once HIFα is brought to the close vicinity of an E3 ligase, it is subjected to polyubiquitination with the aid of an E2 ubiquitin-conjugating enzyme. Polyubiquitin-tagged HIFα is then targeted for 26S proteasome-mediated destruction. In limited oxygen tension or lack of dioxygen cofactor, PHD fails to hydroxylate HIFα. Thus, preventing its recognition by the VHL E3 ligase complex and consequently HIFα escapes destruction. The now-stable HIFα binds constitutively expressed HIFβ/ARNT to form an active HIF transcription factor to activate numerous hypoxia-inducible genes, triggering our physiological responses to hypoxia (1).

The regulation of HIF is further complicated by the fact that under reduced oxygen tension, asparagine remains unhydroxylated (25). This allows transcriptional co-activators CBP/p300 to bind HIF-1α to form an efficient transcriptional complex with ARNT (25). The fact that there are now multiple HIFα subunits as well as multiple posttranslational modifications of HIFα, which are intricately linked to the availability of oxygen, suggest that oxygen homeostasis is not only critical but also complex and requires multiple levels of regulation. Adding to this complexity is our finding that a *VHL*-homologous gene *VLP* encodes a protein that acts as a dominant-negative VHL. Unlike VHL, VLP binds HIF-1α irrespective of its prolyl hydroxylation status and demonstrates no E3 ligase activity on HIF-1α. Because the non-prolyl-hydroxylated HIF-1α is already stable, it is likely that VLP functions to protect VHL-recognizable prolyl-hydroxylated HIF-1α from degradation. This may occur within a precise range of oxygen gradient where the initiation of the hypoxia response would be desirable, but PHD at this level of oxygen may still be capable of hydroxylating HIF-1α. Thus, the stability and accumulation of HIF-1α would depend on the protective function of VLP by competing against VHL. Alternatively, there may be a requirement of VLP for the proper functioning of HIF.

Neovascularization is crucial for proper placental development. During embryogenesis, while VHL is ubiquitously expressed in all three germ cell layers and their derivatives (28, 29), we have observed significant amount of *VLP* transcript in the placenta. Furthermore, the embryonic lethality of *VHL* knockout mice has been attributed to the defective placental vasculogenesis (30). It is tempting to speculate that during placental development, the balance between VHL and VLP is crucial in safeguarding the timely and appropriate level of transcriptional activity of HIF.

Finally, *VLP* locus is located on 1q21.2 between markers D1S2721 and D1S2635. This region of chromosome 1 is frequently associated with renal diseases. For example, t(X;1)(p11;q21) is often observed in renal clear cell carcinomas (RCCs; 31) and *PRCC* (papillary renal cell carcinoma) gene, which forms a fusion product with *TFE3* on Xp11.2, which is mapped downstream of *VLP* on 1q21.2 (32, 33). The chromosomal region between D1S2343 and D1S305, just upstream of *VLP* locus, is linked to the familial papillary thyroid carcinoma/papillary renal neoplasia (fPTC/PRC) phenotype (34). A locus between D1S2696 and D1S2653 on 1q21 is associated with an autosomal dominant form of progressive renal failure and hypertension (35). Furthermore, 1q21-31 is frequently amplified in primary RCCs, especially in metastatic RCCs (36). It will be important to determine whether *VLP* is dysregulated or overexpressed in certain forms of kidney cancer.

Materials and Methods

Gene Cloning

A recent GenBank cDNA entry (Accession No.: XM_089387) encoded a protein similar to VHL. This cDNA sequence mapped to a human genomic DNA sequence from clone RP11-443G18

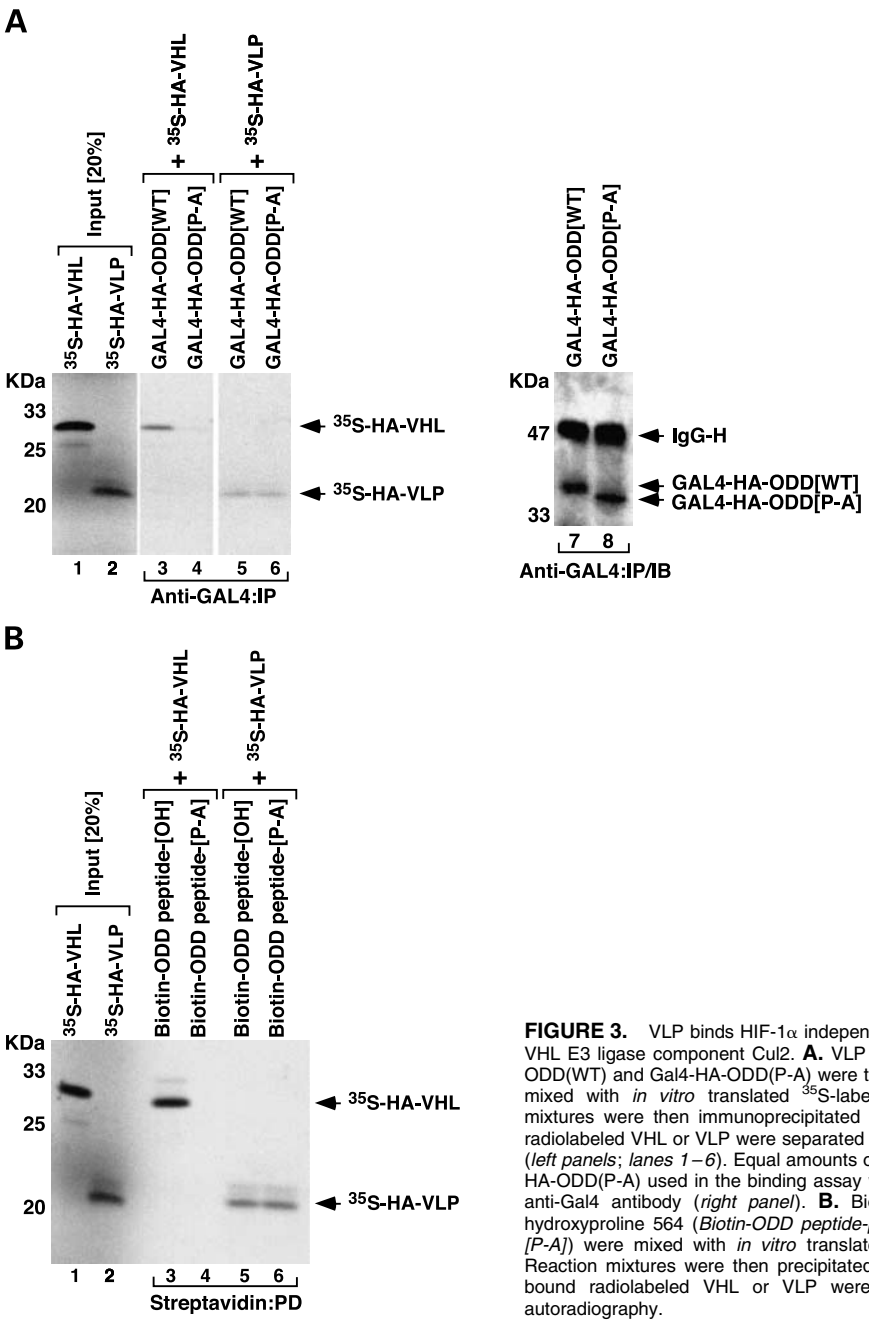

FIGURE 3. VLP binds HIF-1α independent of prolyl hydroxylation status but fails to bind VHL E3 ligase component Cul2. **A.** VLP binds HIF-1α(ODD). *In vitro* translated Gal4-HA-ODD(WT) and Gal4-HA-ODD(P-A) were treated with cellular extracts enriched for PHD and mixed with *in vitro* translated ^{35}S-labeled HA-VHL or ^{35}S-labeled HA-VLP. Reaction mixtures were then immunoprecipitated with anti-Gal4 antibody, and the co-precipitating radiolabeled VHL or VLP were separated on SDS-PAGE and visualized by autoradiography (*left panels*; *lanes 1–6*). Equal amounts of *in vitro* translated Gal4-HA-ODD(WT) and Gal4-HA-ODD(P-A) used in the binding assay were immunoprecipitated and immunoblotted with anti-Gal4 antibody (*right panel*). **B.** Biotinylated HIF-1α residue 556–575 with either hydroxyproline 564 (*Biotin-ODD peptide-[OH]*) or P564A substitution (*Biotin-ODD peptide [P-A]*) were mixed with *in vitro* translated ^{35}S-labeled HA-VHL or ^{35}S-labeled HA-VLP. Reaction mixtures were then precipitated with streptavidin-coated Sepharose beads. The bound radiolabeled VHL or VLP were separated on SDS-PAGE and visualized by autoradiography.

(Accession No.: AL589685) on chromosome 1q21.2 between markers D1S2721 and D1S2635. On the basis of the cDNA and genomic DNA sequences, we performed RT-PCR on total RNA isolated from human brain cerebellum (Clontech, Palo Alto, CA) and cells derived from various tissue types, such as 786-O (kidney), SAOS-2 (bone), HepG2 (liver), and MCF7 (breast). PolyT primer (5′-T_{25}VN-3′, V = G + A + C, N = G + A + T + C) and *VLP*-specific antisense primer (5′-TCA-CTGTGCTCCTG CGTCAGC-3′) were used for the reverse transcription. The reaction without Reverse Transcriptase (SuperScript II H$^-$ from Invitrogen, Carlsbad, CA) was included as negative control. PCR was performed using forward

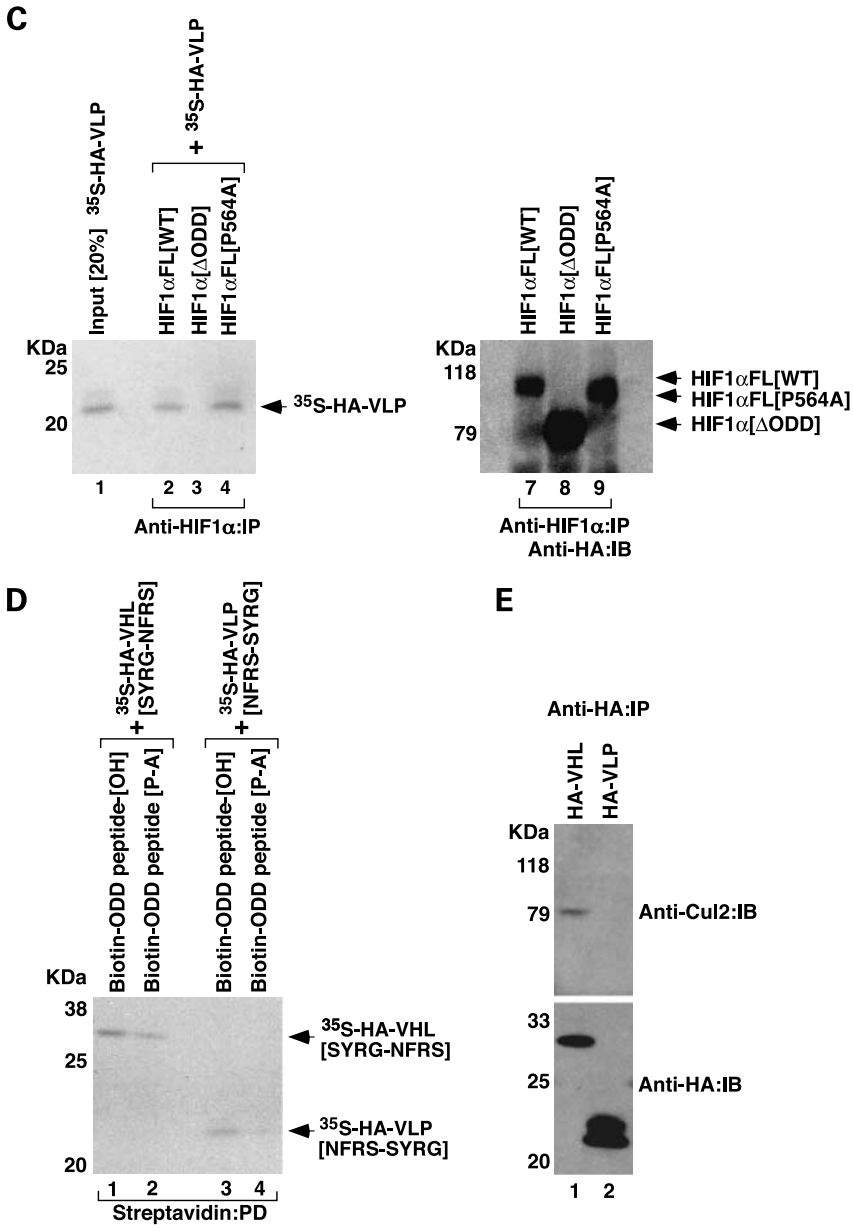

FIGURE 3 *continued.* **C.** VLP binds full-length HIF-1α independent of P564 hydroxylation status. *In vitro* translates of full-length HIF-1α(FL) or HIF-1α[ΔODD] or HIF-1α[P564A] were treated with cellular extracts enriched for PHD and mixed with ^{35}S-labeled HA-VLP. Reaction mixtures were then immunoprecipitated with anti-HIF-1α antibody. Bound proteins were separated on SDS-PAGE and visualized by autoradiography (*left panel*; *lanes 2–4*). Twenty percent input of the radiolabeled VLP is indicated on *lane 1*. *In vitro* translated HIF-1α(FL), HIF-1α(ΔODD), and HIF-1α(P564A) used in the binding assay were immunoprecipitated and immunoblotted with the indicated antibodies (*right panel*). **D.** Biotinylated HIF-1α residue 556–575 with either hydroxyproline 564 (*Biotin-ODD peptide-[OH]*) or P564A substitution (*Biotin-ODD peptide [P-A]*) were mixed with *in vitro* translated ^{35}S-labeled HA-VHL(^{111}SYRG^{114}-NFRS) or ^{35}S-labeled HA-VLP(^{92}NFRS^{95}-SYRG). Reaction mixtures were then precipitated with streptavidin-coated Sepharose beads. The bound radiolabeled VHL(^{111}SYRG^{114}-NFRS) or VLP(^{92}NFRS^{95}-SYRG) were separated on SDS-PAGE and visualized by autoradiography. **E.** VLP fails to bind VHL E3 ligase component Cul2. U2OS osteosarcoma cells were transiently transfected with plasmid encoding either HA-VHL or HA-VLP. Cells were then lysed and immunoprecipitated with anti-HA antibody. Bound proteins were separated on SDS-PAGE and immunoblotted with the indicated antibodies. *IP,* immunoprecipitation; *IB,* immunoblot.

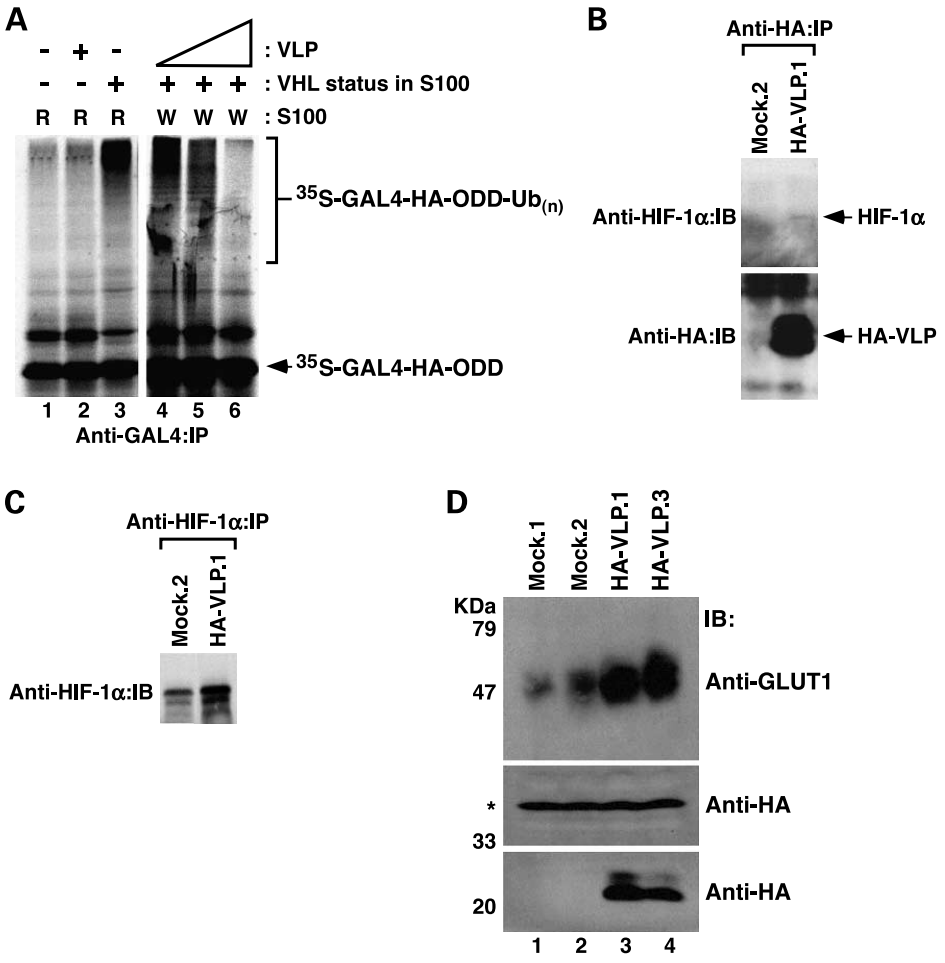

FIGURE 4. VLP acts as a dominant-negative VHL and promotes the accumulation of HIF-1α. **A.** *In vitro* ubiquitination of ^{35}S-labeled HA-hHIF-1α(ODD), treated with cellular extracts enriched for PHD, was performed using S100 extracts generated from 786-O renal carcinoma cells devoid of pVHL (*lanes 1–3*). Reaction mixtures were then reconstituted with *in vitro* translated VHL (2 μl; *lane 3*) or VLP (2 μl; *lane 2*) or mock translate (2 μl; *lane 1*). *In vitro* ubiquitination of ^{35}S-labeled HA-hHIF-1α(ODD), treated with cellular extracts enriched for PHD, was also performed using S100 extracts derived from 786-O renal carcinoma cells ectopically producing VHL (*lanes 3–6*). Reaction mixtures were then supplemented with increasing amounts of *in vitro* translated VLP (2, 4, and 6 μl; represented by a *triangle*). All reaction mixtures were immunoprecipitated with anti-Gal4 antibody. Bound proteins were then separated on SDS-PAGE and visualized by autoradiography. **B.** VLP binds endogenous HIF-1α. U2OS (*VHL*+/+) subclones stably expressing HA-VLP or empty plasmid (*Mock.2*) were lysed under normoxia and immunoprecipitated with an anti-HA antibody. Bound proteins were separated on SDS-PAGE and immunoblotted with the indicated antibodies. **C** and **D.** VLP promotes the accumulation of HIF-1α and GLUT1. **C.** Mock.2 and HA-VLP.1 cells were lysed and 1 mg of whole cell extracts was immunoprecipitated with an excess of anti-HIF-1α antibody. Bound proteins were separated on SDS-PAGE and immunoblotted with an anti-HIF-1α antibody. **D.** Whole cell extracts (100 μg) were separated on SDS-PAGE and immunoblotted with anti-GLUT1 or anti-HA antibody. *Asterisk* indicates a non-specific protein that cross-reacts to the anti-HA antibody, and serves as an internal loading control.

5′-CTCCCAGCCTTTCTGATTCCA-3′ and reverse 5′-TCAC TGTGCTCCTGCGTCAGC-3′ primers. The PCR products were inserted into *Sma*I site of pBluescript II KS (+/−) and sequenced. The partial *VLP* cDNA sequence has been submitted to GenBank (Accession No.: AY494836).

Cells

786-O RCC subclones stably transfected to produce wild-type pVHL or transfected with empty plasmid were as previously described (37, 38). Osteosarcoma U2OS (American Type Culture Collection, Rockville, MD) subclones stably transfected with pcDNA-HA-VLP or empty plasmid were selected under DMEM supplemented with 10% heat-inactivated fetal bovine serum containing G418 (500 μg/ml). Renal carcinoma ACHN cells were obtained from ATCC and cultured in DMEM containing 10% fetal bovine serum. Cells were maintained at 37°C in a humidified 5% CO_2 atmosphere.

Antibodies

Monoclonal anti-Gal4 (DBD; RK5C1) and anti-HA (12CA5) antibodies were from Santa Cruz Biotechnology Inc. (Santa Cruz, CA) and Roche (Indianapolis, IN) respectively. Monoclonal anti-HIF-1α, anti-Cul2, and polyclonal anti-GLUT1 antibodies were obtained from Novus Biologicals (Littleton, CO), Zymed (South San Francisco, CA) and Alpha Diagnostic Intl. Inc. (San Antonio, TX) respectively. Polyclonal (R98) and monoclonal (IG32) anti-VHL antibodies were described previously (38).

Plasmids

The generation of mammalian expression plasmids pRc-CMV-HA-VHL, pcDNA3-HA-HIF-1α(Full-length/P564A/ΔODD), and pcDNA3-Gal4-HA-HIF-1α-ODD(WT/P-A) was described previously (9). To generate pcDNA3-HA-VLP(WT) and pcDNA3-VLP(WT), the ORF of VLP was PCR-amplified using forward primers 5′-GACGACGGATCCCCCTGGA-GAGCGGGGAAC-3′, 5′-GACGACGGATCCATGCCCTG-GAGAGCGGGGAAC-3′ and reverse primer 5′-GACG-ACGAATTCTCAGGGTATACACTGCAGT-3′ and inserted into *Bam*HI/*Eco*RI sites of pcDNA3-HA plasmid. pcDNA3-HA-VHL(^{111}SYRG^{114}-NFRS) and pcDNA3-HA-VLP(^{92}NFRS^{95}-SYRG) were generated using Stratagene QuikChange site-directed mutagenesis kit (La Jolla, CA) and the following primer sets: 5′-CATCCACAACTTCCGAAGTCACCTTTG-3′/5′-CAAAGGT-GACTTCGGAAGTTGTGGATG-3′ and 5′-CTTCCGCATCCA-CAGCTACC-GAGGCCAC CCTTGGCTC-3′/5′-GAGCCAAGGGTGGCCTCGGTAGCTGTGGATGCG--GAGCCAAGGGTGGCCTCGGTAGCTGTGGATGCG-GAAG-3′, respectively. All plasmids made by PCR were confirmed by DNA sequencing.

Northern Blot Analysis

VLP and *VHL* probes for the human multiple tissue northern (MTN) blot (Clontech) were derived from *Bam*HI/*Eco*RI fragments of pcDNA3-HA-VLP and pcDNA3-T7-VHL, respectively, and labeled with ^{32}P-dCTP using the DECAprime II random priming kit (Ambion, Austin, TX). The multiple tissue northern blot was incubated in a hybridization buffer for 30 min and then the labeled probe was added (2×10^6 cpm/ml) for approximately 1 h at 68°C. The membrane was washed 3 times in 2× SSC [0.3 M NaCl, 0.03 M sodium citrate (pH 7.0)] and 0.05% SDS for 30 min, and 2 times in 0.1× SSC, 0.1% SDS at 50°C for 40 min. VLP bands were visualized by autoradiography. β-Actin was subsequently probed as a loading control.

Immunoprecipitation and Immunoblotting

Immunoprecipitation and Western blotting were performed as described previously (39). In brief, cells were lysed in EBC buffer [50 mM Tris (pH 8.0), 120 mM NaCl, 0.5% NP40] supplemented with protease and phosphatase inhibitors (Roche). Immunoprecipitates, immobilized on protein A-Sepharose (Amersham Biosciences, Uppsala, Sweden), were washed 5 times with NETN buffer [20 mM Tris (pH 8.0), 120 mM NaCl, 1 mM ETDA, 0.5% NP40], eluted by boiling in SDS-containing sample buffer, and separated on SDS-PAGE.

Purification of HIF PHD

Extracts containing enriched PHD were purified from rabbit reticulocyte lysate as previously described (13).

In Vitro Binding Assay

Assay for binding of HIF-1α to VHL and VLP was performed as previously described (9, 40). Reticulocyte lysate translation products were synthesized in the presence (for pcDNA3-HA-VHL and pcDNA3-HA-VLP) or absence [for various pcDNA3-HA-HIF-1α(FL), pcDNA3-HA-HIF-1α(ODD), pcDNA3-HA-HIF-1α(P564A), pcDNA3-Gal4-HA-HIF-1α(ODD), and pcDNA3-HA-Gal4-HIF-1α(ODD; P564A)] of ^{35}S-methionine. The various HIF-1α translation products were treated with or without cellular fractions containing enriched PHD for 30 min at 37°C. The various HIF-1α (10 μl) and VHL or VLP (10 μl) translation products were incubated with anti-HIF-1α or anti-Gal4 antibody and protein A-Sepharose in 750 μl of EBC buffer [50 mM Tris (pH 8), 120 mM NaCl, 0.5% NP40]. After five washes with NETN buffer [20 mM Tris (pH 8), 100 mM NaCl, 0.5% NP40, 1 mM EDTA], the bound proteins were resolved on SDS-PAGE and detected by autoradiography. Binding assay of biotinylated HIF-1α residue 556–575 with either hydroxyproline 564 or P564A substitution to VHL or VLP was performed as previously described (12).

In Vitro Ubiquitination Assay

In vitro ubiquitination assay was performed as previously described (9). ^{35}S-methionine-labeled reticulocyte lysate Gal4-HA-HIF-1α(ODD) translation products (4 μl) were incubated in RCC 786-O S100 extracts [100–150 μg; prepared as previously described (9)] supplemented with 8 μg/μl of ubiquitin (Sigma, St. Louis, MO), 100 ng/μl of ubiquitin-aldehyde (BostonBiochem, Cambridge, MA), and an ATP-regenerating system [20 mM Tris (pH 7.4), 2 mM ATP, 5 mM $MgCl_2$, 40 mM creatine phosphate, 0.5 μg/μl of creatine kinase] in a reaction volume of 20–30 μl for 1.5 h at 30°C.

Acknowledgments

We thank the members of the Ohh lab for helpful discussions. We also thank Drs. Ron and Joan Conaway for providing PHD-enriched cellular fractions.

References

1. Leung, S. K. and Ohh, M. Playing tag with HIF: the VHL story. J. Biomed. Biotechnol., *2:* 131–135, 2002.

2. Maher, E. and Kaelin, W. G. von Hippel-Lindau disease. Medicine, *76:* 381–391, 1997.

3. Ang, S. O., Chen, H., Hirota, K., Gordeuk, V. R., Jelinek, J., Guan, Y., Liu, E., Sergueeva, A. I., Miasnikova, G. Y., Mole, D., Maxwell, P. H., Stockton, D. W., Semenza, G. L., and Prchal, J. T. Disruption of oxygen homeostasis underlies congenital Chuvash polycythemia. Nat. Genet., *32:* 614–621, 2002.

4. Ang, S. O., Chen, H., Gordeuk, V. R., Sergueeva, A. I., Polyakova, L. A., Miasnikova, G. Y., Kralovics, R., Stockton, D. W., and Prchal, J. T. Endemic polycythemia in Russia: mutation in the VHL gene. Blood Cells Mol. Dis., *28:* 57–62, 2002.

5. Ivan, M. and Kaelin, W. G. The von Hippel-Lindau tumor suppressor protein. Curr. Opin. Genet. Dev., *11:* 27–34, 2001.

6. Ohh, M. and Kaelin, W. G. J. The von Hippel-Lindau tumour suppressor protein: new perspectives. Mol. Med. Today, *5:* 257–263, 1999.

7. Stebbins, C. E., Kaelin, W. G., and Pavletich, N. P. Structure of the VHL-ElonginC-elonginB complex: implications for VHL tumor suppressor function. Science, *284:* 455–461, 1999.

8. Ohh, M., Takagi, Y., Aso, T., Stebbins, C., Pavletich, N., Zbar, B., Conaway, R., Conaway, J., and Kaelin, W. J. Synthetic peptides define critical contacts between elongin C, elongin B, and the von Hippel-Lindau protein. J. Clin. Invest., *104:* 1583–1591, 1999.

9. Ohh, M., Park, C. W., Ivan, M., Hoffman, M. A., Kim, T-Y., Huang, L. E., Chau, V., and Kaelin, W. G. Ubiquitination of HIF requires direct binding to the von Hippel-Lindau protein β domain. Nat. Cell Biol., *2:* 423–427, 2000.

10. Bruick, R. K. and McKnight, S. L. A conserved family of prolyl-4-hydroxylases that modify HIF. Science, *294:* 1337–1340, 2001.

11. Epstein, A. C., Gleadle, J. M., McNeill, L. A., Hewitson, K. S., O'Rourke, J., Mole, D. R., Mukherji, M., Metzen, E., Wilson, M. I., Dhanda, A., Tian, Y. M.,

Masson, N., Hamilton, D. L., Jaakkola, P., Barstead, R., Hodgkin, J., Maxwell, P. H., Pugh, C. W., Schofield, C. J., and Ratcliffe, P. J. *C. elegans* EGL-9 and mammalian homologs define a family of dioxygenases that regulate HIF by prolyl hydroxylation. [see comments]. Cell, *107:* 43–54, 2001.

12. Ivan, M., Kondo, K., Yang, H., Kim, W., Valiando, J., Ohh, M., Salic, A., Asara, J. M., Lane, W. S., and Kaelin, W. G., Jr. HIFα targeted for VHL-mediated destruction by proline hydroxylation: implications for O_2 sensing. Science, *292:* 464–468, 2001.

13. Ivan, M., Haberberger, T., Gervasi, D. C., Michelson, K. S., Gunzler, V., Kondo, K., Yang, H., Sorokina, I., Conaway, R. C., Conaway, J. W., and Kaelin, W. G., Jr. Biochemical purification and pharmacological inhibition of a mammalian prolyl hydroxylase acting on hypoxia-inducible factor. Proc. Natl. Acad. Sci. USA, *99:* 13459–13464, 2002.

14. Jaakkola, P., Mole, D. R., Tian, Y. M., Wilson, M. I., Gielbert, J., Gaskell, S. J., Kriegsheim, A., Hebestreit, H. F., Mukherji, M., Schofield, C. J., Maxwell, P. H., Pugh, C. W., and Ratcliffe, P. J. Targeting of HIF-α to the von Hippel-Lindau ubiquitylation complex by O_2-regulated prolyl hydroxylation. Science, *292:* 468–472, 2001.

15. Masson, N., Willam, C., Maxwell, P. H., Pugh, C. W., and Ratcliffe, P. J. Independent function of two destruction domains in hypoxia-inducible factor-α chains activated by prolyl hydroxylation. EMBO J., *20:* 5197–5206, 2001.

16. Cockman, M., Masson, N., Mole, D., Jaakkola, P., Chang, G., Clifford, S., Maher, E., Pugh, C., Ratcliffe, P., and Maxwell, P. Hypoxia inducible factor-α binding and ubiquitylation by the von Hippel-Lindau tumor suppressor protein. J. Biol. Chem., *275:* 25733–25741, 2000.

17. Hoffman, M. A., Ohh, M., Yang, H., Klco, J. M., Ivan, M., and Kaelin, W. G., Jr. von Hippel-Lindau protein mutants linked to type 2C VHL disease preserve the ability to downregulate HIF. Hum. Mol. Genet., *10:* 1019–1027, 2001.

18. Gu, Y. Z., Moran, S. M., Hogenesch, J. B., Wartman, L., and Bradfield, C. A. Molecular characterization and chromosomal localization of a third α-class hypoxia inducible factor subunit, HIF3α. Gene Expr., *7:* 205–213, 1998.

19. Hara, S., Hamada, J., Kobayashi, C., Kondo, Y., and Imura, N. Expression and characterization of hypoxia-inducible factor (HIF)-3α in human kidney: suppression of HIF-mediated gene expression by HIF-3α. Biochem. Biophys. Res. Commun., *287:* 808–813, 2001.

20. Makino, Y., Cao, R., Svensson, K., Bertilsson, G., Asman, M., Tanaka, H., Cao, Y., Berkenstam, A., and Poellinger, L. Inhibitory PAS domain protein is a negative regulator of hypoxia-inducible gene expression. Nature, *414:* 550–554, 2001.

21. Makino, Y., Kanopka, A., Wilson, W. J., Tanaka, H., and Poellinger, L. IPAS is an hypoxia-inducible splicing variant of the HIF-3α locus. J. Biol. Chem., *277:* 32405–32408, 2002.

22. Maynard, M. A., Qi, H., Chung, J., Lee, E. H., Kondo, Y., Hara, S., Conaway, R. C., Conaway, J. W., and Ohh, M. Multiple splice variants of the human HIF-3α locus are targets of the VHL E3 ubiquitin ligase complex. J. Biol. Chem., *278:* 11032–11040, 2003.

23. Semenza, G. Perspectives on oxygen sensing. Cell, *98:* 281–284, 1999.

24. Semenza, G. HIF-1 and human disease: one highly involved factor. Genes Dev., *14:* 1983–1991, 2000.

25. Lando, D., Peet, D. J., Whelan, D. A., Gorman, J. J., and Whitelaw, M. L. Asparagine hydroxylation of the HIF transactivation domain a hypoxic switch. Science, *295:* 858–861, 2002.

26. Bradley, J. F. and Rothberg, P. G. Processed pseudogene from the von Hippel-Lindau disease gene is located on human chromosome 1. Diagn. Mol. Pathol., *8:* 101–106, 1999.

27. Min, J. H., Yang, H., Ivan, M., Gertler, F., Kaelin, W. G., Jr., and Pavletich, N. P. Structure of an HIF-1α-pVHL complex: hydroxyproline recognition in signaling. Science, *296:* 1886–1889, 2002.

28. Gnarra, J. R., Duan, D. R., Weng, Y., Humphrey, J. S., Chen, D. Y. T., Lee, S., Pause, A., Dudley, C. F., Latif, F., Kuzmin, I., Schmidt, L., Duh, F-M., Stackhouse, T., Chen, F., Kishida, T., Wei, M. H., Lerman, M. I., Zbar, B., Kalusner, R. D., and Linehan, W. M. Molecular cloning of the von Hippel-Lindau tumor suppressor gene and its role in renal cell carcinoma (Review). Biochim. Biophys. Acta, *1242:* 201–210, 1996.

29. Kessler, P., Vasavada, S., Rackley, R., Stackhouse, T., Duh, F., Latif, F., Lerman, M., Zbar, B., and Williams, B. Expression of the von Hippel-Lindau tumor-suppressor gene, VHL, in human fetal kidney and during mouse embryogenesis. Mol. Med., *1:* 457–466, 1995.

30. Gnarra, J., Ward, J., Porter, F., Wagne, J., Devor, D., Grinberg, A., Emmert-Buck, M., Westphal, H., Klausner, R., and Linehan, W. Defective placental vasculogenesis causes embryonic lethality in VHL-deficient mice. Proc. Natl. Acad. Sci. USA, *94:* 9102–9107, 1997.

31. Weterman, M. A., Wilbrink, M., Dijkhuizen, T., van den Berg, E., and Geurts van Kessel, A. Fine mapping of the 1q21 breakpoint of the papillary renal cell carcinoma-associated (X;1) translocation. Hum. Genet., *98:* 16–21, 1996.

32. Sidhar, S. K., Clark, J., Gill, S., Hamoudi, R., Crew, A. J., Gwilliam, R., Ross, M., Linehan, W. M., Birdsall, S., Shipley, J., and Cooper, C. S. The t(X;1)(p11.2;q21.2) translocation in papillary renal cell carcinoma fuses a novel gene PRCC to the TFE3 transcription factor gene. Hum. Mol. Genet., *5:* 1333–1338, 1996.

33. Weterman, M. A., Wilbrink, M., and Geurts van Kessel, A. Fusion of the transcription factor *TFE3* gene to a novel gene, *PRCC*, in t(X;1)(p11;q21)-positive papillary renal cell carcinomas. Proc. Natl. Acad. Sci. USA, *93:* 15294–15298, 1996.

34. Malchoff, C. D., Sarfarazi, M., Tendler, B., Forouhar, F., Whalen, G., Joshi, V., Arnold, A., and Malchoff, D. M. Papillary thyroid carcinoma associated with papillary renal neoplasia: genetic linkage analysis of a distinct heritable tumor syndrome. J. Clin. Endocrinol. Metab., *85:* 1758–1764, 2000.

35. Cohn, D. H., Shohat, T., Yahav, M., Ilan, T., Rechavi, G., King, L., and Shohat, M. A locus for an autosomal dominant form of progressive renal failure and hypertension at chromosome 1q21. Am. J. Hum. Genet., *67:* 647–651, 2000.

36. Gronwald, J., Storkel, S., Holtgreve-Grez, H., Hadaczek, P., Brinkschmidt, C., Jauch, A., Lubinski, J., and Cremer, T. Comparison of DNA gains and losses in primary renal clear cell carcinomas and metastatic sites: importance of 1q and 3p copy number changes in metastatic events. Cancer Res., *57:* 481–487, 1997.

37. Iliopoulos, O., Kibel, A., Gray, S., and Kaelin, W. G. Tumor suppression by the human von Hippel-Lindau gene product. Nat. Med., *1:* 822–826, 1995.

38. Kibel, A., Iliopoulos, O., DeCaprio, J. D., and Kaelin, W. G. Binding of the von Hippel-Lindau tumor suppressor protein to elongin B and C. Science, *269:* 1444–1446, 1995.

39. Ohh, M., Yauch, R. L., Lonergan, K. M., Whaley, J. M., Stemmer-Rachamimov, A. O., Louis, D. N., Gavin, B. J., Kley, N., Kaelin, W. G., Iliopoulos, O., and Kaelin, W. G. The von Hippel-Lindau tumor suppressor protein is required for proper assembly of an extracellular fibronectin matrix. Mol. Cell, *1:* 959–968, 1998.

40. Ohh, M., Kim, W. Y., Moslehi, J. J., Chen, Y., Chau, V., Read, M. A., and Kaelin, W. G. An intact NEDD8 pathway is required for Cullin-dependent ubiquitylation in mammalian cells. EMBO Rep., *3:* 177–182, 2002.